Cancer Immunology, Immunotherapy (2020) 69:745–758
https://doi.org/10.1007/s00262-020-02508-9

ORIGINAL ARTICLE

Activation of TLR4 signaling inhibits progression of osteosarcoma by stimulating CD8-positive cytotoxic lymphocytes

Kenichiro Yahiro[1] · Yoshihiro Matsumoto[1] · Hisakata Yamada[1] · Makoto Endo[1] · Nokitaka Setsu[1] · Toshifumi Fujiwara[1] · Makoto Nakagawa[1,2] · Atsushi Kimura[1] · Eijiro Shimada[1] · Seiji Okada[3] · Yoshinao Oda[4] · Yasuharu Nakashima[1]

Received: 13 August 2019 / Accepted: 28 January 2020 / Published online: 11 February 2020

Abstract

Background Osteosarcoma (OS) is the most common malignant bone tumor and the prognosis of advanced cases is still poor. Recently, there have been several reports suggesting the relationship between innate immunity and OS, but the detailed mechanism is unknown. We demonstrate the relationship between OS and Toll-like receptor 4 (TLR4) which is one of the most important factors in innate immunity.

Methods We established a syngenic mouse tumor model using C3H/HeN, C3H/HeJ mouse and a highly metastatic OS cell line, LM8. TLR4 activation with lipopolysaccharide (LPS) was performed on both mice and its influence on the progression of OS was evaluated. We also performed CD8 + cells depletion to examine the influence on TLR4 activation effects.

Results Tumor volume of C3H/HeN mice was significantly smaller and overall survival of C3H/HeN mice was significantly longer than C3H/HeJ mice. We found more CD8+ cells infiltrating in lung metastases of C3H/HeN mice and depletion of CD8+ cells canceled the antitumor effects of LPS.

Conclusion TLR4 activation by LPS increased CD8+ cells infiltrating into lung metastases and suppressed OS progression in the mouse model. TLR4 activation may suppress the progression of OS via stimulating CD8+ cells and can be expected as a novel treatment for OS.

Keywords Osteosarcoma · Toll-like receptor 4 · Innate immunity · CD8-positive lymphocytes · Prognosis

Abbreviations

CLP	Liposomal clodronate
LPS	Lipopolysaccharide
OAS	Overall survival
OS	Osteosarcoma
PFS	Progression-free survival
S.D	Standard deviation
TAM	Tumor-associated macrophage
TLR	Toll-like receptor

Introduction

Osteosarcoma (OS) is the most common malignant bone tumor. The prognosis of OS has greatly improved due to the use of adjuvant and neoadjuvant chemotherapy [1], but patients with advanced disease marked by distant metastasis still have a poor prognosis and the development of new treatment strategies would be highly beneficial.

Electronic supplementary material The online version of this article (https://doi.org/10.1007/s00262-020-02508-9) contains supplementary material, which is available to authorized users.

✉ Yoshihiro Matsumoto
ymatsu@ortho.med.kyushu-u.ac.jp

[1] Department of Orthopaedic Surgery, Graduate School of Medical Sciences, Kyushu University, 3-1-1, Maidashi, Higashi-ku, Fukuoka, Fukuoka, Japan

[2] Division of Orthopaedic Surgery, National Cancer Center Hospital, 5-1-1, Tsukiji, Chuo-ku, Tokyo, Japan

[3] Department of Immunobiology and Neuroscience Medical. Medical Institute of Bioregulation, Kyushu University, 3-1-1, Maidashi, Higashi-ku, Fukuoka, Fukuoka, Japan

[4] Department of Anatomic Pathology, Pathological Sciences, Graduate School of Medical Sciences, Kyushu University, 3-1-1, Maidashi, Higashi-ku, Fukuoka, Fukuoka, Japan

A recent study showed that malignant tumors were able to continue growing, because they had escaped detection by the host immune system [2]. Prevention of this immune escape may inhibit the progression of malignant tumors. Advancements in immunotherapy such as anti–PD-1 antibody and chimeric antigen receptor T cells have improved the prognosis of various cancers [3, 4]; however, the efficacy of immunotherapy for OS remains to be determined [5].

The immune system consists of two defense mechanisms that interact with each other to protect the host: innate immunity and acquired immunity. Innate immunity is nonspecific and functions soon after encountering a potential threat; its main effector cells include macrophages, dendritic cells, and natural killer cells. Acquired immunity functions later and is antigen-specific; its main effector cells include cytotoxic T cells and plasma cells. Innate immunity has been reported to inhibit tumorigenesis and tumor growth [6]. Mifamurtide (MEPACT®), a drug that stimulates host innate immunity, improves the survival of OS patients [7, 8] and is approved for patients with non-metastatic OS in Europe. Although the underlying mechanism remains unknown, activation of innate immunity may exert an antitumor effect in patients with OS.

Toll-like receptors (TLRs) are a family of pattern recognition receptors that play an important role in innate immunity by recognizing pathogens. Stimulated TLRs initiate signal transduction pathways that activate various transcription factors such as IRF and NF-κB and induce the production of proinflammatory cytokines including TNFα and IFNγ. In particular, TLR4 recognizes lipopolysaccharide (LPS), a major component of the outer membrane of Gram-negative bacteria, and induces inflammation to inhibit bacterial proliferation [9]. An association between bacterial infection and OS progression has previously been described, and studies in dogs and humans have reported better prognoses for patients with OS who developed wound infection after surgery [10, 11]. In addition, in a mouse model of OS with chronic staphylococcal osteomyelitis, the growth of OS was significantly suppressed by osteomyelitis [12]. Bacterial proliferation activates TLR4, suggesting a relationship between TLR4 and OS, but the detailed mechanism is unknown.

The role of TLR4 signaling in the progression of malignant tumors is controversial; activation of TLR4 results in an antitumor effect in glioma [13], but promotes tumor growth in hepatocellular carcinoma [14]. We developed a syngeneic mouse model of OS to investigate the role of TLR4 signaling in the progression of OS.

Materials and methods

Cell culture

LM8 was maintained in Dulbecco's Modified Eagle's Medium (DMEM, Thermo Fisher Scientific, Waltham, MA, USA) supplemented with 10% fetal bovine serum (HyClone Laboratories, Logan, UT, USA), 100 units/ml penicillin, and 100 µg/ml streptomycin at 37 °C in an atmosphere of 5% CO_2.

Reagents

Lipopolysaccharide (LPS, O55:B5) and monophosphoryl lipid A (MPL, Minnesota Re595) were purchased from Sigma-Aldrich (St. Louis, MO, USA). Dulbecco's phosphate-buffered saline (PBS) was purchased from Thermo Fisher Scientific. LPS and MPL were dissolved in PBS.

Syngeneic mouse model

Four-week-old female C3H/HeN and C3H/HeJ mice (11–15 g) were maintained in a pathogen-free environment with a 12-h dark/light cycle in the animal facility at Kyushu University. Five animals per cage were housed and all animals were fed and watered ad libitum. Animal health was checked at least twice a week to visually assess appearance behavior, feces and other conditions. The mice were anesthetized by a mixed cocktail of midazolam (Fuji Pharma Co., Ltd., Tokyo, Japan), butorphanol tartrate (Meiji Seika Pharma Co., Ltd., Tokyo, Japan) and medetomidine hydrochloride (Kyoritsu Seiyaku Corp., Tokyo, Japan). The mice were randomly assigned to the experiments.

1×10^6 LM8 cells were dissolved in 100 µl Matrigel® (Corning, Corning, NY, USA) and injected subcutaneously (s.c.) into the backs of mice on day 0. Beginning 3 days after tumor injection, mice were administered 100 µl of 1 mg/ml lipopolysaccharide (LPS; Sigma-Aldrich) or 100 µl PBS (DPBS; Thermo Fisher Scientific) intraperitoneally (i.p.) every 7 days. The tumor size was measured weekly by calipers, and the tumor volume was calculated using the following formula: (major axis of tumor) × (minor axis of tumor)^2/2. The overall survival time of the mice was also assessed.

Moderate tumor size and LPS administration did not seem to have a major effect on the mouse's well-being. Because large tumor adversely affected the behavior and appearance of mice, and the burden on mice was too large, mice with tumors exceeding 20 mm in the major axis and/

or with severe emaciation were euthanized by cervical dislocation after anesthesia.

In vivo depletion of CD8$^+$ T cells

Mice were depleted of CD8$^+$ T cells by intraperitoneal administration of anti-CD8a antibody (YTS169.4, rat IgG2b; BioXCell, West Lebanon, NH, USA). Each mouse was administered 100 µg anti-CD8a antibody or control rat IgG2b (BioLegend, San Diego, CA, USA) at 3 days and 1 day prior to tumor implantation and weekly thereafter. The efficiency of T-cell depletion was evaluated by flow cytometry. Three days after tumor implantation, tumor-bearing CD8-depleted mice and control mice were administered 100 µg LPS or 100 µl PBS once a week, respectively. The tumor size was measured weekly and the overall survival time was assessed as previously described.

In vivo depletion of tumor-associated macrophages

Mice were depleted of macrophages by the intraperitoneal administration of liposomal clodronate (Clophosome®; FormuMax Scientific, Sunnyvale, CA, USA) (CLP). Each mouse was administered 200 µl of CLP or PBS 3 days prior to tumor implantation and 100 µl CLP every 4 days thereafter. The efficiency of macrophage depletion was confirmed by flow cytometry. Beginning 3 days after tumor implantation, tumor-bearing macrophage-depleted mice and control mice were administered 100 µg LPS once per week. The tumor size was measured weekly using a caliper and the overall survival time of the mice was assessed as previously described.

Isolation of CD11b$^+$ cells

CD11b$^+$ cells were isolated from LM8 tumors via magnetic sorting using CD11b MicroBeads (Miltenyi Biotec, Bergisch, Gladbach, Germany) as described previously [15]. LM8 tumors were excised and minced in 10 ml DMEM with collagenase L (Nitta Gelatin, Osaka, Japan) and DNase I (F. Hoffman-La Roche AG, Basel, Switzerland). The mixture was incubated for 30 min at 37 °C and digestion was halted by the addition of fetal bovine serum. The cell suspension was washed and passed through a 70-µm mesh nylon screen and then incubated with CD11b MicroBeads for 15 min at 4 °C. CD11b$^+$ cells were isolated using an autoMACS separator (Miltenyi Biotec). CD11b$^+$ cells isolated from tumors were used as tumor-associated macrophages for further experiments.

Flow cytometry

Flow cytometry experiments for in vivo CD8$^+$ cell depletion were performed on a BD Accuri™ C6 flow cytometer (BD Biosciences, San Jose, CA, USA). Blood was drawn from the heart and splenocytes were collected by mincing the excised spleen with scissors and an 18G needle. Red blood cells were lysed using BD Pharm Lyse prior to monoclonal antibody staining. Each sample was blocked using Anti-mouse C16/CD32 antibody (BD Pharmingen) and stained with the following primary antibodies: CD3-FITC clone 17A2, CD4-PE clone GK1.5, and CD8a-APC clone 53–6.7 (MD Biosciences, Oakdale, MN, USA). After 15-min incubation, each sample was washed with PBS containing 2% fetal bovine serum and analyzed by flow cytometry. A flow cytometry analysis of in vivo macrophage depletion was performed using CD11b-FITC and F4/80-APC primary antibodies (Miltenyi Biotec). We excised the LM8 tumors and prepared a single-cell suspension as well as isolated CD11b$^+$ cells. These single-cell suspensions were incubated for 15 min at 4 °C with the fluorescently labeled antibodies described above and subsequently analyzed by flow cytometry. The experiments were performed in triplicate.

Quantitative reverse transcription polymerase chain reaction (RT-PCR)

RNA was extracted using an RNeasy Mini Kit (Qiagen, Hilden, Germany) and reverse transcribed using a PrimeScript™ RT reagent Kit (Takara Bio, Tokyo, Japan. Real-time quantitative PCR was performed using a LightCycler 1.5 (Perfect Real Time, Takara Bio) with SYBR Green reagent (Takara Bio). The expression of inducible nitric oxide synthase (*iNOS*), MHC class 2 (*MHC2*), and arginase-1 (*Arg1*) was assessed using the following primers:

iNOS (forward: 5′-CAAGCACCTTGGAAGAGGAG-3′, reverse: 5′-AAGGCCAAACACAGCATACC-3′), *MHC2* (forward: 5′-GACGCTCAACTTGTCCCAAAAC-3′, reverse: 5′-GCAGCCGTGAACTTGTTGAAC-3′), *Arg1* (forward: 5′-TCACCTGAGCTTTGATGTCG-3′, reverse: 5′-CTGAAAGGAGCCCTGTCTTG-3′). Data were standardized using GAPDH as a reference gene. Assays were performed in triplicate.

Enzyme-linked immunosorbent assay (ELISA)

Mouse splenocytes were harvested as previously mentioned. Mouse peritoneal macrophages were harvested by administering 10 ml cold PBS intraperitoneally into C3H/HeJ and C3H/HeN mice, followed by gentle abdominal massage and withdrawal of the fluid. The collected peritoneal fluid was centrifuged for 5 min at 1000 rpm to collect peritoneal macrophages and the supernatant was discarded.

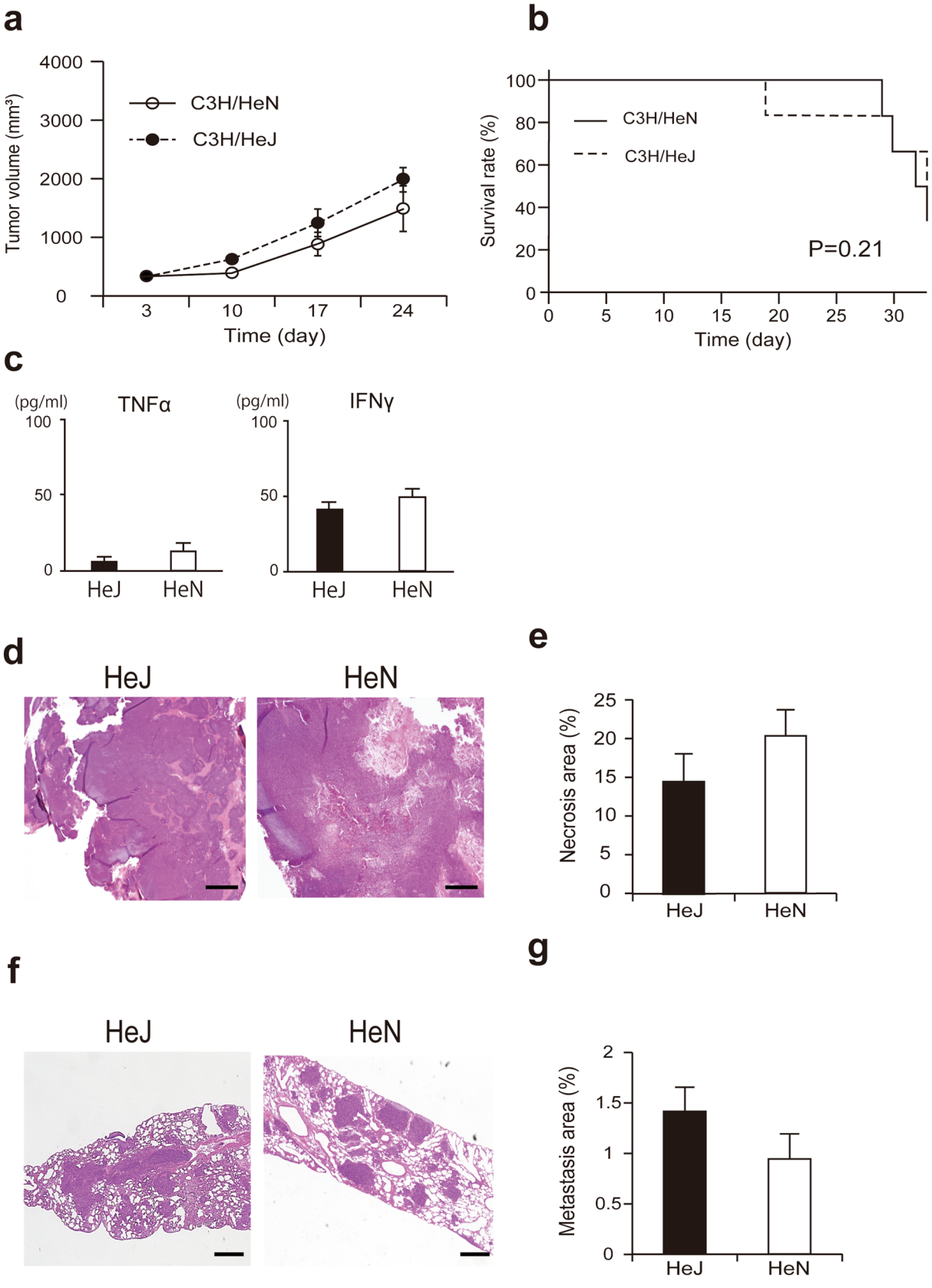
a
Tumor volume (mm³)
4000
3000
2000
1000
0
C3H/HeN
C3H/HeJ
3
10
17
24
Time (day)
b
Survival rate (%)
100
80
60
40
20
0
C3H/HeN
C3H/HeJ
P=0.21
0
5
10
15
20
25
30
Time (day)
c
(pg/ml)
TNFα
100
50
0
HeJ
HeN
(pg/ml)
IFNγ
100
50
0
HeJ
HeN
d
HeJ
HeN
e
Necrosis area (%)
25
20
15
10
5
0
HeJ
HeN
f
HeJ
HeN
g
Metastasis area (%)
2
1.5
1
0.5
0
HeJ
HeN

◂**Fig. 1** In the absence of TLR4 stimulation, there was no significant difference in LM8 OS growth between C3H/HeN and C3H/HeJ mice. **a** LM8 tumor volume curves in C3H/HeN and C3H/HeJ mice without TLR4 stimulation ($n=5$). The white circle solid line indicates C3H/HeN and the black circle dotted line indicates C3H/HeJ. Values represent means ± S.D. MΦ: macrophage. **b** Kaplan–Meier curves for overall survival probability of C3H/HeN and C3H/HeJ mice with LM8 tumors ($n=5$). **c** Serum concentration of TNFα and IFNγ in C3H/HeN ($n=5$) and C3H/HeJ mice ($n=5$) without TLR4 stimulation. Values represent means ± S.D. **d** H&E stain of LM8 tumors, with C3H/HeJ shown in the left panel and C3H/HeN in the right panel. **e** Percentage of necrotic area in tumor tissue ($n=5$). Values represent means ± S.D. Scale bar = 500 μm. **f** H&E stain of LM8 lung metastases, with C3H/HeJ shown in the left panel and C3H/HeN in the right panel. **g** Percentage of metastasis area in lung ($n=5$). Values represent means ± S.D. Scale bar = 200 μm

Mouse peritoneal macrophages were seeded into a 6-well plate at a density of 1×10^5 cells per well. Cells were incubated for 6 h with PBS, 50 ng/ml LPS or 50 ng/ml MPL, and then culture supernatants were collected and used for ELISAs. ELISAs were performed using the Mouse TNF-alpha Quantikine ELISA Kit (R & D Systems, Minneapolis, MN, USA) and the Mouse IFN-gamma Quantikine ELISA Kit (R & D Systems). Assays were performed in triplicate.

Immunohistochemistry

All samples were fixed in 4% paraformaldehyde (FUJIFILM Wako Pure Chemical Corp., Osaka, Japan) and embedded in paraffin. After being deparaffinized in xylene and dehydrated in a graded ethanol series, sections were pretreated with 1.0 nM EDTA (FUJIFILM Wako) in a microwave oven at 100 °C for 15 min before incubation with primary antibody at 4 °C overnight. The following primary antibodies were used: CD8 antibody (C8/144B, DAKO Denmark A/S, Glostrup, Denmark) and F4/80 antibody (ab100790, Abcam, Cambridge, UK). Samples were then incubated with Dako EnVision Dual Link System-HRP (Agilent), visualized using the diaminobenzidine substrate system (FUJIFILM Wako), and counterstained with diluted hematoxylin.

All images were captured and analyzed using a BZ-X810 microscope (Keyence, Osaka, Japan). The Hybrid Cell Count system of the microscope was used to quantify the necrotic area in the tumors and the metastatic area in the lung as well as to count immunostained cells in the tissue. The necrotic area was quantified by calculating the area ratio of the necrotic area in the maximum plane of the tumor. The metastatic area was quantified by calculating the area ratio of OS cells in a lung lobe. Immunostain-positive cells were quantified by calculating the area ratio of positive cells in a lung lobe.

Clinical OS samples

Clinical samples were obtained from OS lung metastases that had been surgically resected from 13 patients between 1996 and 2018 at the Graduate School of Medical Science, Kyushu University, Fukuoka, Japan. In each case, a diagnosis of OS was made on the basis of histologic features. The samples were analyzed by immunohistochemistry with various antibodies. The Institutional Review Board at Kyushu University approved the use of human specimens for this study.

Statistical analyses

The Mann–Whitney *U* test was used for two-group comparisons, with $P<0.05$ considered to be statistically significant. Data in graphs are shown as means ± standard deviation (S.D.). A generalized Wilcoxon test was used to generate Kaplan–Meier survival estimates for the syngeneic mouse model and clinical OS samples. $P<0.05$ was considered to be statistically significant. All statistical analyses were performed using the Statistical Analysis System (SAS) software package (JMP12 Pro; SAS Institute, Cary, NC, USA).

Results

Generation of a syngeneic mouse model for OS

To investigate whether host TLR4 signaling affects the progression of OS, we established a syngeneic mouse model of OS by transplanting cells from the highly metastatic mouse OS cell line LM8 [16] into C3H mice. It is important to note that there are two distinctive strains of C3H mice, C3H/HeJ and C3H/HeN. C3H/HeJ mice have a mutation in the TLR4 gene such that TLR4 is nonfunctional and does not respond to LPS stimulation [17], whereas C3H/HeN mice have functional TLR4 and are sensitive to LPS stimulation.

We transplanted 1×10^6 LM8 cells subcutaneously into C3H/HeN and C3H/HeJ mice to establish the OS tumor. Nearly all LM8 cells transplanted into both mouse strains were successfully established and metastasized to the lungs. Mice survived for 4–6 weeks after transplantation of LM8 cells. Importantly, there were no significant differences in the tumor volume or overall survival (OAS) between C3H/HeN and C3H/HeJ mice (Fig. 1a, b). TNFα and IFNγ are representative cytokines induced by TLR4 activation and we found no significant differences in their serum concentrations between C3H/HeN and C3H/HeJ mice (Fig. 1c). We evaluated the necrotic area in tumor and the rate of lung metastasis (Fig. 1d, f) and found that in C3H/HeN mice, the necrotic area in the tumor was slightly wider and the rate of lung metastasis was slightly

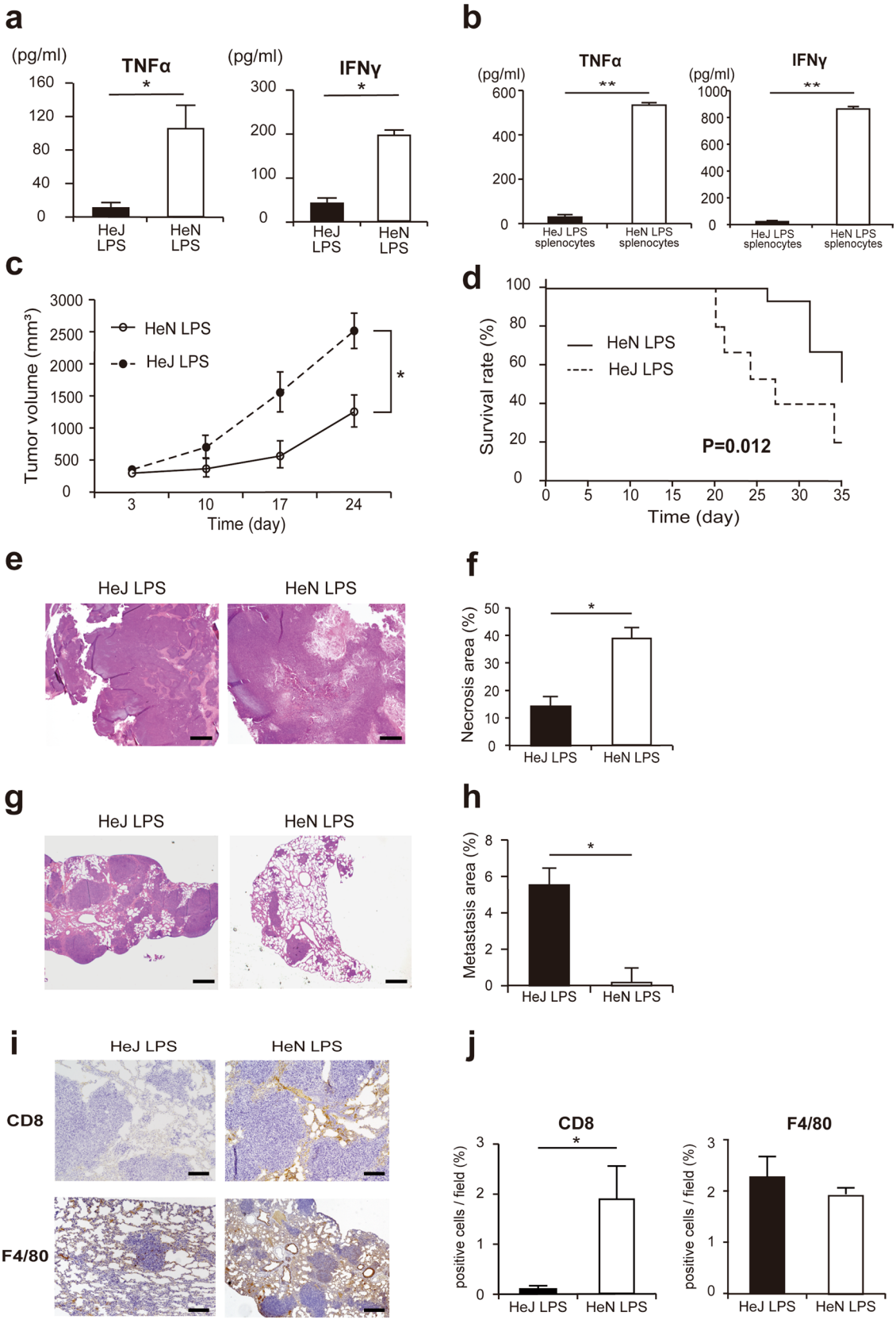
a
(pg/ml)
TNFα
160
120
80
40
0
*
HeJ LPS
HeN LPS
(pg/ml)
IFNγ
300
200
100
0
*
HeJ LPS
HeN LPS
b
(pg/ml)
TNFα
600
400
200
0
**
HeJ LPS splenocytes
HeN LPS splenocytes
(pg/ml)
IFNγ
1000
800
600
400
200
0
**
HeJ LPS splenocytes
HeN LPS splenocytes
c
Tumor volume (mm³)
3000
2500
2000
1500
1000
500
0
HeN LPS
HeJ LPS
*
3
10
17
24
Time (day)
d
Survival rate (%)
100
80
60
40
20
0
HeN LPS
HeJ LPS
P=0.012
0
5
10
15
20
25
30
35
Time (day)
e
HeJ LPS
HeN LPS
f
Necrosis area (%)
50
40
30
20
10
0
*
HeJ LPS
HeN LPS
g
HeJ LPS
HeN LPS
h
Metastasis area (%)
8
6
4
2
0
*
HeJ LPS
HeN LPS
i
HeJ LPS
HeN LPS
CD8
F4/80
j
CD8
positive cells / field (%)
3
2
1
0
*
HeJ LPS
HeN LPS
F4/80
positive cells / field (%)
3
2
1
0
HeJ LPS
HeN LPS

◂**Fig. 2** In the presence of TLR4 stimulation, C3H/HeN mice show less growth of LM8 cells than C3H/HeJ mice. **a** Serum concentrations of TNFα and IFNγ in C3H/HeN and C3H/HeJ mice 6 h after LPS administration ($n=5$). Values represent means ± S.D. $*P<0.05$ by Mann–Whitney U test. **b** Measurement of TNFα and IFNγ concentration in culture supernatants by ELISA 24 h after LPS administration to splenocytes from C3H/HeN and C3H/HeJ mice ($n=5$). Values represent means ± S.D. $**P<0.01$ by Mann–Whitney U test. **c** LM8 tumor volume curve in C3H/HeN and C3H/HeJ mice with LPS-induced TLR4 stimulation ($n=10$). Dotted line indicates C3H/HeJ mice treated with LPS and solid line indicates C3H/HeN mice treated with LPS. Values represent means ± S.D. $*P<0.05$ by Mann–Whitney U test. **d** Kaplan–Meier curves for overall survival probability of C3H/HeN and C3H/HeJ mice with LM8 tumors after LPS administration ($n=10$). The dotted line indicates C3H/HeJ and the solid line indicates C3H/HeN. A generalized Wilcoxon test was used for statistical analysis. **e** H&E stain of LM8 tumors, with C3H/HeJ in the left panel and C3H/HeN in the right panel. **f** Percentage of necrotic area in tumor tissue ($n=10$). Values represent means ± S.D. $*P<0.05$ by Mann–Whitney U test. Scale bar = 500 µm. **g** H&E stain of LM8 lung metastases, with C3H/HeJ in the left panel and C3H/HeN in the right panel. **h** Percentage of metastasis area in lung ($n=10$). Values represent means ± S.D. $*P<0.05$ by Mann–Whitney U test. Scale bar = 200 µm. **i** Immunohistochemical staining of LM8 lung metastases of C3H/HeJ (left) and C3H/HeN (right) mice. Upper panels show CD8 staining and lower panels show F4/80 staining. Scale bars = 200 µm. **j** The percentage of $CD8^+$ (left) and $F4/80^+$ (right) cells in a lobe ($n=10$). Values represent means ± S.D. $*P<0.05$ by Mann–Whitney U test

smaller than in C3H/HeJ mice, but the differences were not significant (Fig. 1e, g). These results suggest that the presence of functional TLR4 does not significantly affect the progression of OS in this model.

LPS-induced activation of TLR4 inhibits the progression of mouse osteosarcoma

To examine whether TLR4 activation affects the progression of OS, we injected mice with LPS 3 days after transplantation of LM8 cells. First, to confirm the LPS-induced activation of TLR4 signaling, we evaluated the serum levels of TNFα and IFNγ. As expected, in vivo LPS administration increased the serum levels of TNFα and IFNγ in C3H/HeN mice but not in C3H/HeJ mice (Fig. 2a). Similarly, cytokine production in response to ex vivo LPS administration to isolated splenocytes was observed only in cells from C3H/HeN mice (Fig. 2b). We observed that C3H/HeN mice treated with LPS had a significantly smaller tumor volume than C3H/HeJ mice and their OAS was significantly longer (Fig. 2c, d). Histologically, tumors in C3H/HeN mice had significantly larger necrotic areas than those in C3H/HeJ mice (Fig. 2e, f). In addition, C3H/HeN mice treated with LPS had significantly lower rates of lung metastasis than C3H/HeJ mice (Fig. 2g, h). Taken together, these results suggest that LPS-induced activation of TLR4 inhibits the progression of OS.

TLR4 activation increases tumor infiltration by $CD8^+$ cells

Next, we sought to investigate the mechanism by which the LPS-induced activation of TLR4 inhibits OS progression. Activation of TLR4 signaling induces inflammation by promoting the release of inflammatory cytokines, followed by the activation of various immune cells. To determine which immune cells might confer antitumor effects after LPS administration, we performed immunohistochemical staining for $CD8^+$ T cells and $F4/80^+$ macrophages (macrophages) in tumor and lung metastasis tissue.

In both C3H/HeN and C3H/HeJ mice, $CD8^+$ T cells and macrophages surrounded the transplanted tumors but did not appear to infiltrate them. When we examined lung tissue, however, we observed considerable infiltration of $CD8^+$ T cells in tumors of C3H/HeN mice, but few $CD8^+$ T cells in tumors of C3H/HeJ mice (Fig. 2i, j). Macrophages infiltrated tumors in mice of both genotypes and we observed no significant differences (Fig. 2i, j).

$CD8^+$ cells are required for TLR4 activation to have an antitumor effect

Our results led us to hypothesize that $CD8^+$ T cells or macrophages might play an important role in tumor suppression brought about by LPS-induced TLR4 activation. To investigate the role of $CD8^+$ T cells in OS, we performed in vivo depletion of $CD8^+$ T cells in C3H/HeN and C3H/HeJ mice. We intraperitoneally administered a neutralizing anti-CD8 antibody or isotype control prior to transplantation of LM8 cells and depletion of $CD8^+$ T cells was confirmed by flow cytometry (Fig. 3a). Depletion of $CD8^+$ T cells caused serum TNFα and IFNγ levels to decrease significantly (Fig. 3b). Furthermore, the depletion of $CD8^+$ T cells negated the LPS-induced suppression of tumor growth and extension of OAS (Fig. 3c, d) in C3H/HeN mice. We observed an increase in the tumor volume in C3H/HeJ mice, without a significant effect on OAS (Fig. 3c, e). Histologically, the depletion of $CD8^+$ T cells increased the necrotic area in tumors (Fig. 3f, g) and the area of lung metastasis in C3H/HeN mice (Fig. 3h, i). These data suggest that $CD8^+$ T cells are necessary for LPS-induced activation of TLR4 signaling to inhibit OS progression.

To better understand the effects of LPS and CD8+ T cells in C3H/HeN mice, we also performed in vivo depletion of CD8+ T cells in LPS-untreated mice (Supplementary Fig. 1a). The tumor size was significantly larger in LPS-untreated CD8-depleted C3H/HeN mice than in LPS-untreated or LPS-treated C3H/HeN mice. The tumor size was also significantly larger in LPS-untreated C3H/HeN mice than in LPS-treated C3H/HeN mice. The OAS was significantly shorter in LPS-untreated CD8-depleted

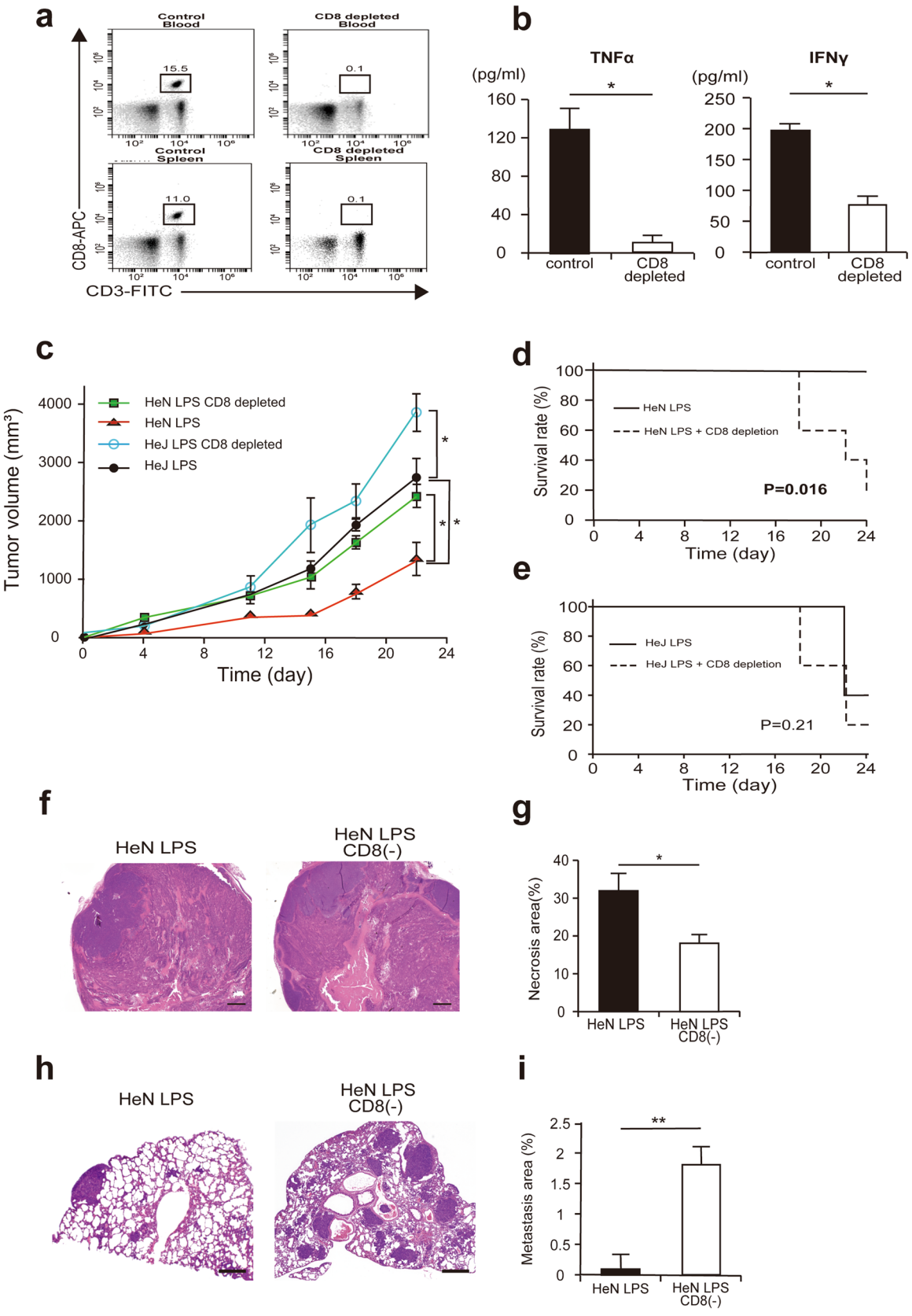
a
Control Blood
CD8 depleted Blood
15.5
0.1
Control Spleen
CD8 depleted Spleen
11.0
0.1
CD8-APC
CD3-FITC
b
TNFα
IFNγ
(pg/ml)
control
CD8 depleted
c
HeN LPS CD8 depleted
HeN LPS
HeJ LPS CD8 depleted
HeJ LPS
Tumor volume (mm³)
Time (day)
d
HeN LPS
HeN LPS + CD8 depletion
P=0.016
Survival rate (%)
Time (day)
e
HeJ LPS
HeJ LPS + CD8 depletion
P=0.21
f
HeN LPS
HeN LPS CD8(-)
g
Necrosis area(%)
h
i
Metastasis area (%)

◂**Fig. 3** Depletion of $CD8^+$ cells abrogates the antitumor effect of TLR4 stimulation. **a** Flow cytometry analysis of blood and spleen confirmed that $CD8^+$ T cells were absent from mice 4 days after administration of anti-CD8 antibody. Data represent representative of three independent experiments. **b** Serum TNFα and IFNγ concentrations in control C3H/HeN mice and $CD8^+$-depleted C3H/HeN mice 6 h after LPS administration ($n=5$). Values represent means ± S.D. $^*P<0.05$ by Mann–Whitney U test. **c** LM8 tumor volume curve in C3H/HeN LPS (red), $CD8^+$-depleted C3H/HeN LPS (green), C3H/HeJ LPS (black), and $CD8^+$-depleted C3H/HeJ LPS (blue) mice ($n=5$). All mice were administered LPS weekly. Values represent means ± S.D. $^*P<0.05$ by Mann–Whitney U test. **d** Kaplan–Meier curves for overall survival probability of C3H/HeN LPS and $CD8^+$-depleted C3H/HeN LPS mice with LM8 tumors ($n=5$). Generalized Wilcoxon test was used for statistical analysis. **e** Kaplan–Meier curves for overall survival probability of C3H/HeJ LPS and $CD8^+$-depleted C3H/HeJ LPS mice with LM8 tumors ($n=5$). Generalized Wilcoxon test was used for statistical analysis. **f** H&E stain of LM8 tumors in C3H/HeN LPS (left) and $CD8^+$-depleted C3H/HeN LPS (right) mice. **g** Percentage of necrotic area in tumor tissue ($n=5$). Values represent means ± S.D. $^*P<0.05$ by Mann–Whitney U test. Scale bar = 500 μm **h** H&E stain of LM8 lung metastases in C3H/HeN LPS (left) and $CD8^+$-depleted C3H/HeN LPS (right) mice. **i** Percentage of metastasis area in lung ($n=5$). Values represent means ± S.D. $^{**}P<0.01$ by Mann–Whitney U test. Scale bar = 200 μm

C3H/HeN mice than in LPS-untreated C3H/HeN mice (Supplementary Fig. 1b) and OAS was slightly shorter in LPS-untreated C3H/HeN mice than in LPS-treated C3H/HeN mice (Supplementary Fig. 1c).

Tumor-associated macrophages (TAMs) are another candidate immune cell type that might regulate LPS-induced activation of TLR4 signaling and several studies have shown an association between TAM and OS [18, 19]. First, we characterized tumor-infiltrating TAMs. There are two types of TAMs, proinflammatory M1 macrophages and anti-inflammatory M2 macrophages; the activation of TLR4 has been reported to induce TAM differentiation to M1 macrophages. We extracted TAMs from C3H/HeN and C3H/HeJ mice after LPS administration and examined the expression of representative markers for M1 and M2 macrophages. We observed no clear tendency toward differentiation into M1 macrophages in either mouse strain (Supplementary Fig. 2a). We then depleted macrophages by administering CLP. We confirmed the depletion of macrophages using flow cytometry (Supplementary Fig. 2b) and found that CLP administration did not affect the serum cytokine level (Supplementary Fig. 2c) or tumor suppression by LPS-induced TLR4 activation in C3H/HeN mice (Supplementary Fig. 2d). TAMs do not appear to play a dominant role in mediating the antitumor effects of LPS-induced TLR4 activation, at least in our model system.

Monophosphoryl lipid A (MPL) inhibits tumor growth in C3H/HeN mice

Although our results clearly show the inhibitory effects of LPS-induced TLR4 activation on OS progression, LPS is too toxic to apply clinically. MPL, a component of LPS, is known to act as a TLR4 agonist and is less toxic than LPS [20]. MPL has been approved as a vaccine adjuvant, confirming its safety in a clinical setting [21]. To test the efficacy of MPL as a TLR4 agonist, we treated cultured mouse macrophages with MPL and measured the concentration of TNFα in the cell culture supernatant. MPL increased the secretion of TNFα from macrophages derived from C3H/HeN mice, but not from C3H/HeJ-derived macrophages (Fig. 4a). In vivo administration of MPL resulted in slightly lower cytokine production relative to LPS, but caused an increase in serum cytokine levels (Fig. 4b). MPL inhibited the growth and lung metastasis of LM8 cells in C3H/HeN mice but not in C3H/HeJ mice (Fig. 4c). MPL also prolonged the survival of C3H/HeN mice after transplantation of LM8 and this effect was not observed in C3H/HeJ mice (Fig. 4d). A histological examination of tumor and lung tissue showed no significant difference in the necrotic area of the tumor (Fig. 4e, f), but the lung metastasis area was significantly smaller in C3H/HeN mice than in C3H/HeJ mice after the administration of MPL (Fig. 4g, h). These results show that MPL is as effective as LPS at activating TLR4 signaling and inhibiting the progression of OS.

$CD8^+$ T cells in lung metastases may predict the prognosis of OS patients

LPS-induced TLR4 activation increased the number of $CD8^+$ T cells in lung metastases and improved the OAS of C3H/HeN mice, implying that infiltration of $CD8^+$ T cells in lung metastases of OS patients might improve their prognosis. To test this hypothesis, we performed immunohistochemical staining on clinical samples derived from lung metastases of OS patients. A summary of the patients' clinical data is shown in Supplementary Table 1. We used antibodies to CD8 and the macrophage marker CD68 and found that the progression-free survival (PFS) (Fig. 5a) of patients with extensive infiltration of $CD8^+$ T cells was significantly longer than that of patients with limited CD8+ T-cell infiltration (Fig. 5b, high CD8 group PFS, 18.6 ± 5.4 months; low CD8 group PFS, 6.63 ± 3.4 months; $P=0.036$). The OAS was not significantly different between the groups (Fig. 5c; high CD8 group OAS, 88.8 ± 17.9 months; low CD8 group OAS, 58.6 ± 5.6 months; $P=0.67$). In addition, there was no clear association between the number of $CD68^+$ cells infiltrating lung metastases and PFS (Fig. 5d; high CD68 group PFS, 13.0 ± 4.3 months; low CD68 group PFS, 5.8 ± 3.8 months; $P=0.5$) or OAS (Fig. 5e; high CD68

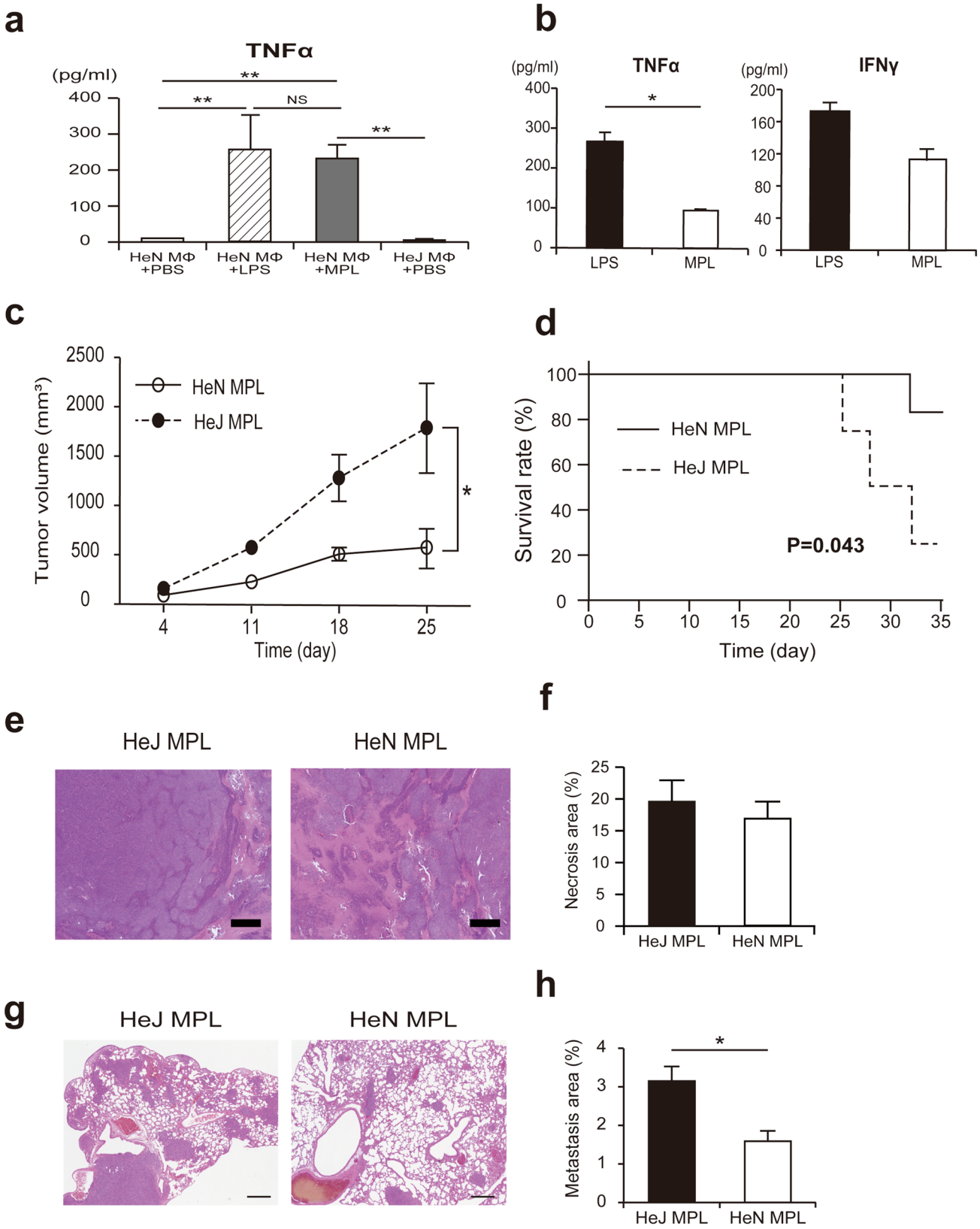
a
TNFα
(pg/ml)
400
300
200
100
0
**
**
NS
**
HeN MΦ +PBS
HeN MΦ +LPS
HeN MΦ +MPL
HeJ MΦ +PBS
b
(pg/ml)
TNFα
400
300
200
100
0
*
LPS
MPL
(pg/ml)
IFNγ
200
160
120
80
40
0
LPS
MPL
c
Tumor volume (mm³)
2500
2000
1500
1000
500
0
HeN MPL
HeJ MPL
*
4
11
18
25
Time (day)
d
Survival rate (%)
100
80
60
40
20
0
HeN MPL
HeJ MPL
P=0.043
0
5
10
15
20
25
30
35
Time (day)
e
HeJ MPL
HeN MPL
f
Necrosis area (%)
25
20
15
10
5
0
HeJ MPL
HeN MPL
g
HeJ MPL
HeN MPL
h
Metastasis area (%)
4
3
2
1
0
*
HeJ MPL
HeN MPL

◂**Fig. 4** MPL is an effective TLR4 agonist with antitumor effects comparable to LPS in C3H/HeN mice. **a** TNFα secretion from primary cultures of intraperitoneal macrophages ($n=3$). Values represent means ± S.D. $^{**}P<0.01$ by Mann–Whitney *U* test. **b** Serum concentrations of TNFα and IFNγ in C3H/HeN mice 6 h after LPS or MPL administration ($n=3$). Values represent means ± S.D. $^{*}P<0.05$ by Mann–Whitney *U* test. **c** LM8 tumor volume curves of C3H/HeN (solid line) and C3H/HeJ (dotted line) mice after MPL treatment ($n=5$). Values represent means ± S.D. $^{*}P<0.05$ by Mann–Whitney *U* test. **d** Kaplan–Meier curves for overall survival probability of C3H/HeN and C3H/HeJ mice with LM8 tumors ($n=5$). A generalized Wilcoxon test was used for statistical analysis. **e** H&E stain of LM8 tumors in C3H/HeJ (left) and C3H/HeN (right) mice treated with MPL. **f** Percentage of necrotic area in tumor tissue ($n=5$). Values represent means ± S.D. Scale bar = 200 µm. **g** H&E stain of LM8 lung metastases in C3H/HeJ (left) and C3H/HeN (right) mice treated with MPL. **h** Percentage of metastasis area in lung ($n=5$). Values represent means ± S.D. $^{*}P<0.05$ by Mann–Whitney *U* test. Scale bar = 200 µm

group OAS, 77.8 ± 11.5 months; low CD68 group OAS, 76.4 ± 21.3 months; $P=0.881$). We also compared PFS and OAS between the CD8/CD68 double high group and other group, but found no significant difference (Supplementary Fig. 3 $P=0.45$ and 0.91 respectively). These results are in agreement with the results of our mouse experiments and suggest that $CD8^+$ T cells may also play an important role in limiting the progression of OS in humans.

Discussion

Modern immunotherapy is based on the observation that systemic infection and subsequent activation of innate immunity can inhibit tumor growth [22]. In the case of OS, several reports have shown a positive effect of systemic infection on the growth of OS. In dogs with OS, localized osteomyelitis after limb-sparing surgery results in a significantly longer PFS than in dogs without infection [10]. In addition, at 10 years after the initial diagnosis, the overall survival rate of OS patients who had an infection within 1 year of implantation surgery was significantly higher than that of non-infected patients and the infection was an independent prognostic factor [11]. These observations suggest that innate immunity may promote antitumor activity in OS patients, but this hypothesis had not previously been explicitly tested.

We first showed that the administration of LPS inhibited tumor growth and prolonged the survival in our syngeneic mouse model of OS. Because TLR4 and its downstream signaling pathway play dominant roles in the LPS-induced activation of innate and adaptive immune responses, we speculated that the activation of TLR4 was critical for LPS to exert its antitumor effect. Consistent with this notion, LPS treatment increased serum concentrations of IFNγ and TNF-α, which are known to be upregulated by the activation of TLR4 signaling [23]. Furthermore, the lack of activation of TLR4 in C3H/HeJ mice prevented LPS from having an antitumor effect.

Several recent reports showed that the degree of intratumoral $CD8^+$ T cell infiltration at the diagnosis of OS is strongly correlated with a better outcome and would be a reliable biomarker for therapeutic stratification [19, 24–26]. This suggests that intratumoral $CD8^+$ T cells play a dominant role in delaying the progression of OS. Remarkably, the number of $CD8^+$ T cells in the lung metastases was increased by LPS administration in C3H/HeN mice. In vivo depletion of $CD8^+$ T cells abrogated the antitumor effect of LPS treatment. We posit that $CD8^+$ T cells are critical mediators of OS growth control associated with the LPS-induced activation of TLR4 signaling.

The growth rate of OS was increased by depletion of $CD8^+$ cells even in LPS-untreated C3H/HeN and C3H/HeJ mice, suggesting that $CD8^+$ T cells might play an additional role in inhibiting progression of OS apart from TLR4 signaling, possibly in an endogenous host reaction. In keeping with this, we found that the PFS of OS patients who had undergone lung metastasectomy was positively correlated with high intratumoral infiltration of $CD8^+$ T cells. In lung cancer, a positive correlation has been observed between the number of $CD8^+$ T cells infiltrating a tumor and the efficacy of immune checkpoint inhibitors [25]. Conventional chemotherapy and radiotherapy may indirectly stimulate host immunity, including T-cell immune responses [27, 28]. Therefore, a combination therapy of TLR4 stimulation with immune checkpoint inhibitors and/or conventional therapy may have a synergistic effect in patients with advanced OS.

Although LPS-based immunotherapy would be effective for patients with advanced OS, LPS treatment also causes severe systemic side effects including fever, fatigue, chills, and myalgia. To address this limitation, multiple natural and synthetic derivatives and analogues of LPS have been tested [23]. MPL, one of the most promising derivatives of LPS, is less toxic in humans than LPS [20]. Intratumoral injection of MPL has been shown to be as effective as LPS in terms of tumor regression, with less toxicity [29]. Unfortunately, MPL administration did not increase the necrotic area. This may be related to the lower cytokine elevation relative to LPS. However, it was considered to be a useful drug because suppression of lung metastasis, which significantly affects the prognosis and improvement in survival rates, was observed. MPL has gone through several preclinical and clinical stages and is FDA-approved for clinical application as an adjuvant for hepatitis B vaccine [21, 30, 31]. In our syngeneic mouse model of OS, MPL inhibited disease progression, and we believe that it has great potential as active immunotherapy for patients with advanced OS.

A recent study reported that the immune infiltrate in OS is mainly composed of TAMs [32]. Other studies have

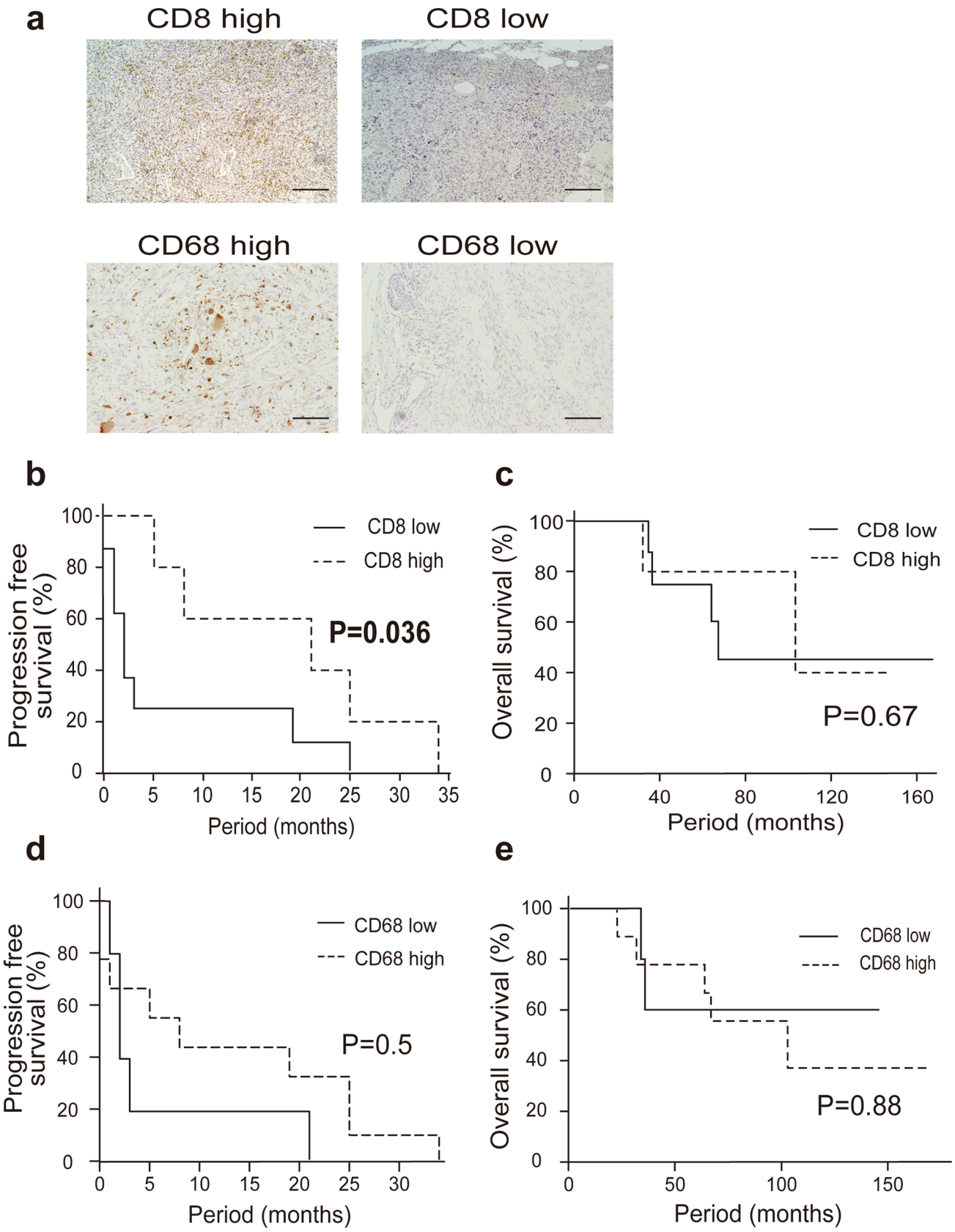
a
CD8 high
CD8 low
CD68 high
CD68 low
b
Progression free survival (%)
CD8 low
CD8 high
P=0.036
Period (months)
c
Overall survival (%)
CD8 low
CD8 high
P=0.67
Period (months)
d
Progression free survival (%)
CD68 low
CD68 high
P=0.5
Period (months)
e
Overall survival (%)
CD68 low
CD68 high
P=0.88
Period (months)

◂**Fig. 5** The number of $CD8^+$ T cells in lung metastases of OS patients correlates with progression-free survival time. **a** Representative images of CD8 and CD68 immunohistochemical staining. Upper left: high CD8 ($n=5$), upper right: low CD8 ($n=8$), lower left: high CD68 ($n=8$), lower right: low CD68 ($n=5$). Scale bar = 500 µm. **b** Kaplan–Meier curves for progression-free survival probability of OS patients. The solid line represents the low CD8 group ($n=8$) and the dotted line represents the high CD8 group ($n=5$). (CD8 high group PFS; 18.6 ± 5.4 months, CD8 low group PFS; 6.63 ± 3.4 months. $P=0.036$). A generalized Wilcoxon test was used for statistical analysis. **c** Kaplan–Meier curves for overall survival probability of OS patients. The solid line represents the low CD8 group ($n=8$) and the dotted line represents the high CD8 group ($n=5$). (CD8 high group OS; 88.8 ± 17.9 months, CD8 low group OS; 58.6 ± 5.6 months. $P=0.67$). A generalized Wilcoxon test was used for statistical analysis. **d** Kaplan–Meier curves for progression-free survival probability of OS patients. The solid line represents the low CD68 group ($n=5$) and the dotted line represents the high CD68 group ($n=8$). (CD68 high group PFS; 13.0 ± 4.3 months, CD68 low group PFS; 5.8 ± 3.8 months. $P=0.5$). A generalized Wilcoxon test was used for statistical analysis. **e** Kaplan–Meier curves for overall survival probability of OS patients. The solid line represents the low CD8 group ($n=5$) and the dotted line represents the high CD8 group ($n=8$). (CD68 high group OS; 77.8 ± 11.5 months, CD68 low group PFS; 76.4 ± 21.3 months. $P=0.881$). A generalized Wilcoxon test was used for statistical analysis

suggested that infiltration of TAMs is associated with reduced metastasis and an improved survival in high-grade OS [18, 33]. Another recent study showed that the presence of $CD163^+$ M2-polarized macrophages is a favorable biomarker for the therapeutic stratification of primary OS patients, indicating that TAMs may have antitumor activity in OS. Surprisingly, we found that depletion of macrophages did not significantly affect cytokine production or tumor growth due to LPS-induced TLR4 activation. This may have been due to insufficient removal of macrophages by CLP, or perhaps because other immune cells such as natural killer, dendritic, or CD4 + cells can compensate for macrophages in processes such as phagocytosis, antigen presentation, and cytokine production. While CLP treatment suppresses tumor growth by eliminating proinflammatory TAMs in Ewing's sarcoma and pancreatic cancer [15, 34], CLP had no significant effect on OS in our model.

Several limitations associated with the present study warrant mention. First, we evaluated only one method of LPS treatment, weekly administration of a 100-µg dose. LPS has been reported to be lethal to mice at a high dose (approximately 25 mg/kg). Although the dose of LPS administered in this experiment was relatively low (approximately 5 mg/kg), it may still cause pathological conditions similar to septic shock, resulting in organ damage and a negative impact on the survival rate. To decrease the negative effects as much as possible while maintaining the effectiveness of LPS, it will be necessary to perform further experiments to determine the dose–response curve of LPS. Second, although TLR4 signaling may activate other immune cells involved in innate immunity, such as dendritic cells and NK cells, we did not evaluate their role in LPS-induced tumor suppression. NK cells are a typical effector of innate immunity and have been reported recently to be useful for cancer immunotherapy [35], therefore, their role in LPS-induced tumor suppression is of particular interest. Finally, the number of OS clinical samples we were able to obtain was too small to draw solid conclusions about the association of $CD8^+$ T-cell infiltration with the clinical prognosis.

In conclusion, our findings suggest that LPS-induced activation of TLR4 may trigger an antitumor immune response to OS and $CD8^+$ T cells are necessary for this response. $CD8^+$ T cells may also affect the progression of OS in humans. Agents that activate $CD8^+$ T cells, including anti–PD-1 antibody and TLR4 agonists such as LPS and MPL, may be promising treatments for patients with advanced OS.

Acknowledgements We thank Dr. Tetsuzo Tagawa from Department of Surgery and Science, Graduate School of Medical Sciences, Kyushu University for kindly providing clinical samples of the patients with OS.

Author contributions KY, YM, and HY designed research; KY, AK, and ES performed research; YM, HY, EM, NS, and TF analyzed data; MN, SO, YO, and YN supervised research; KY and YM drafted the manuscript.

Funding This work was supported by Grants-in-Aid for Young Scientists (18K16627, 19K16802), Grant-in-Aid for Scientific Research (18K09067) from the Japan Society for the Promotion of Science, a Grant from Japan Orthopedics and Traumatology Research Foundation Inc. (No. 332). Toshifumi Fujiwara was also recipient of Fukuoka Foundation for Sound Health Cancer Research Fund.

Compliance with ethical standards

Conflict of interest The authors declare no conflict of interest.

Ethics approval and ethical standards The study was conducted in accordance with the Declaration of Helsinki and approved by the Institutional Ethical Review Board of the Kyushu University (#27–420, 2016/3/31). The animal study was approved by the Institutional Ethical Review Board of the Kyushu University (#A28-160–0, 2017–3-31). Experiments involving animals were performed in compliance with the guidelines established by the Animal Care and Use Committee and this study was approved by the Institutional Review Board at Kyushu University.

Informed consent Prior to the use of patient data and specimens in the study, written informed consent was obtained from all patients. They all agreed to use their clinical data and bio materials for this research and publication. Written informed consent was obtained also from the parents when the patient was a minor.

Animal source C3H/HeN and C3H/HeJ mice were purchased from Kyudo (Saga, Japan).

Cell line authentication LM8 mouse osteosarcoma cells were purchased from RIKEN BioResource Research Center (Tsukuba, Japan). Cell line authentication of LM8 was performed by RIKEN.

References

1. Iwamoto Y et al (2009) Multiinstitutional phase II study of neoadjuvant chemotherapy for osteosarcoma (NECO study) in Japan: NECO-93J and NECO-95J. J Orthop Sci 14(4):397–404
2. Teng MW et al (2015) From mice to humans: developments in cancer immunoediting. J Clin Invest 125(9):3338–3346
3. Wolchok JD et al (2017) Overall survival with combined nivolumab and ipilimumab in advanced melanoma. N Engl J Med 377(14):1345–1356
4. Byrd TT et al (2018) TEM8/ANTXR1-specific CAR T cells as a targeted therapy for triple-negative breast cancer. Cancer Res 78(2):489–500
5. Heumann D, Roger T (2002) Initial responses to endotoxins and Gram-negative bacteria. Clin Chim Acta 323(1–2):59–72
6. Hagerling C, Casbon AJ, Werb Z (2015) Balancing the innate immune system in tumor development. Trends Cell Biol 25(4):214–220
7. Wycislo KL, Fan TM (2015) The immunotherapy of canine osteosarcoma: a historical and systematic review. J Vet Intern Med 29(3):759–769
8. Jimmy R et al (2017) Effectiveness of mifamurtide in addition to standard chemotherapy for high-grade osteosarcoma: a systematic review. JBI Database System Rev Implement Rep 15(8):2113–2152
9. Molteni M, Gemma S, Rossetti C (2016) The role of Toll-Like receptor 4 in infectious and noninfectious inflammation. Mediators Inflamm 2016:6978936
10. Lascelles BD et al (2005) Improved survival associated with postoperative wound infection in dogs treated with limb-salvage surgery for osteosarcoma. Ann Surg Oncol 12(12):1073–1083
11. Jeys LM et al (2007) Post operative infection and increased survival in osteosarcoma patients: are they associated? Ann Surg Oncol 14(10):2887–2895
12. Sottnik JL et al (2010) Chronic bacterial osteomyelitis suppression of tumor growth requires innate immune responses. Cancer Immunol Immunother 59(3):367–378
13. Han S et al (2017) LPS alters the immuno-phenotype of glioma and glioma stem-like cells and induces in vivo antitumor immunity via TLR4. J Exp Clin Cancer Res 36(1):83
14. Yao RR et al (2018) M2-polarized tumor-associated macrophages facilitated migration and epithelial-mesenchymal transition of HCC cells via the TLR4/STAT3 signaling pathway. World J Surg Oncol 16(1):9
15. Fujiwara T et al (2011) Macrophage infiltration predicts a poor prognosis for human ewing sarcoma. Am J Pathol 179(3):1157–1170
16. Asai T et al (1998) Establishment and characterization of a murine osteosarcoma cell line (LM8) with high metastatic potential to the lung. Int J Cancer 76(3):418–422
17. Poltorak A et al (1998) Defective LPS signaling in C3H/HeJ and C57BL/10ScCr mice: mutations in Tlr4 gene. Science 282(5396):2085–2088
18. Buddingh EP et al (2011) Tumor-infiltrating macrophages are associated with metastasis suppression in high-grade osteosarcoma: a rationale for treatment with macrophage activating agents. Clin Cancer Res 17(8):2110–2119
19. Gomez-Brouchet A et al (2017) CD163-positive tumor-associated macrophages and CD8-positive cytotoxic lymphocytes are powerful diagnostic markers for the therapeutic stratification of osteosarcoma patients: an immunohistochemical analysis of the biopsies fromthe French OS2006 phase 3 trial. Oncoimmunology 6(9):e1331193
20. Baldridge JR et al (2004) Taking a Toll on human disease: Toll-like receptor 4 agonists as vaccine adjuvants and monotherapeutic agents. Expert Opin Biol Ther 4(7):1129–1138
21. Vacchelli E et al (2012) Trial watch: FDA-approved Toll-like receptor agonists for cancer therapy. Oncoimmunology 1(6):894–907
22. Coley WB (1893) A preliminary note on the treatment of inoperable sarcoma by the toxic product of erysipelas. Post-Graduate 8:278–286
23. Shetab Boushehri MA, Lamprecht A (2018) TLR4-based immunotherapeutics in cancer: a review of the achievements and shortcomings. Mol Pharm 15(11):4777–4800
24. Matsuo T et al (2009) Extraskeletal osteosarcoma with partial spontaneous regression. Anticancer Res 29(12):5197–5201
25. Haratani K et al (2017) Tumor immune microenvironment and nivolumab efficacy in EGFR mutation-positive non-small-cell lung cancer based on T790M status after disease progression during EGFR-TKI treatment. Ann Oncol 28(7):1532–1539
26. Fritzsching B et al (2015) CD8(+)/FOXP3(+)-ratio in osteosarcoma microenvironment separates survivors from non-survivors: a multicenter validated retrospective study. Oncoimmunology 4(3):e990800
27. Park JY et al (2009) Doxorubicin enhances CD4(+) T-cell immune responses by inducing expression of CD40 ligand and 4–1BB. Int Immunopharmacol 9(13–14):1530–1539
28. Galluzzi L et al (2015) Immunological effects of conventional chemotherapy and targeted anticancer agents. Cancer Cell 28(6):690–714
29. Won EK et al (2003) Analysis of the antitumoral mechanisms of lipopolysaccharide against glioblastoma multiforme. Anticancer Drugs 14(6):457–466
30. Adams S (2009) Toll-like receptor agonists in cancer therapy. Immunotherapy 1(6):949–964
31. Ribi E et al (1984) Lipid A and immunotherapy. Rev Infect Dis 6(4):567–572
32. Inagaki Y et al (2016) Dendritic and mast cell involvement in the inflammatory response to primary malignant bone tumours. Clin Sarcoma Res 6:13
33. Dumars C et al (2016) Dysregulation of macrophage polarization is associated with the metastatic process in osteosarcoma. Oncotarget 7(48):78343–78354
34. Griesmann H et al (2017) Pharmacological macrophage inhibition decreases metastasis formation in a genetic model of pancreatic cancer. Gut 66(7):1278–1285
35. Rezvani K et al (2017) Engineering natural killer cells for cancer immunotherapy. Mol Ther 25(8):1769–1781